Application of deep convolutional neural network for automated detection of myocardial infarction using ECG signals

U. Rajendra Acharya [a,b,c], Hamido Fujita [d,*], Shu Lih Oh [a], Yuki Hagiwara [a], Jen Hong Tan [a], Muhammad Adam [a]

[a] Department of Electronics and Computer Engineering, Ngee Ann Polytechnic, Singapore
[b] Department of Biomedical Engineering, School of Science and Technology, Singapore University of Social Sciences, Singapore
[c] Department of Biomedical Engineering, Faculty of Engineering, University of Malaya, Malaysia
[d] Iwate Prefectural University (IPU), Faculty of Software and Information Science, Iwate 020-0693, Japan

ARTICLE INFO

ABSTRACT

The electrocardiogram (ECG) is a useful diagnostic tool to diagnose various cardiovascular diseases (CVDs) such as myocardial infarction (MI). The ECG records the heart's electrical activity and these signals are able to reflect the abnormal activity of the heart. However, it is challenging to visually interpret the ECG signals due to its small amplitude and duration. Therefore, we propose a novel approach to automatically detect the MI using ECG signals. In this study, we implemented a convolutional neural network (CNN) algorithm for the automated detection of a normal and MI ECG beats (with noise and without noise). We achieved an average accuracy of 93.53% and 95.22% using ECG beats with noise and without noise removal respectively. Further, no feature extraction or selection is performed in this work. Hence, our proposed algorithm can accurately detect the unknown ECG signals even with noise. So, this system can be introduced in clinical settings to aid the clinicians in the diagnosis of MI.

© 2017 Elsevier Inc. All rights reserved.

1. Introduction

Myocardial infarction (MI) is caused when the blood flow to a segment of the myocardium is disrupted [4,27]. Coronary arteries are the arteries that supply oxygen-rich blood to the heart muscle. However, if there is a blockage of the coronary artery due to the buildup of plaques, it reduces the blood flow to the heart muscle. That segment of the heart muscle will start to die if blood flow is not restored in time [27]. Fig. 1 illustrates the myocardial infarction due to the blockage of a coronary artery. This artery gets blocked with blood clots also known as a thrombus. These blood clots are formed due to the plaque build-up in the artery. The complete blockage of blood flow results in a heart attack as a part of the heart muscle is damaged [21].

Furthermore, MI is also often referred to as the silent heart attack. It is because patients are not aware that they are suffering from MI until a heart attack occurs. According to the American Health Association, it is estimated that *750,000* Americans have a heart attack every year. Out of these 750,000 Americans, 210,000 of them have a recurrent heart at-

* Corresponding author.
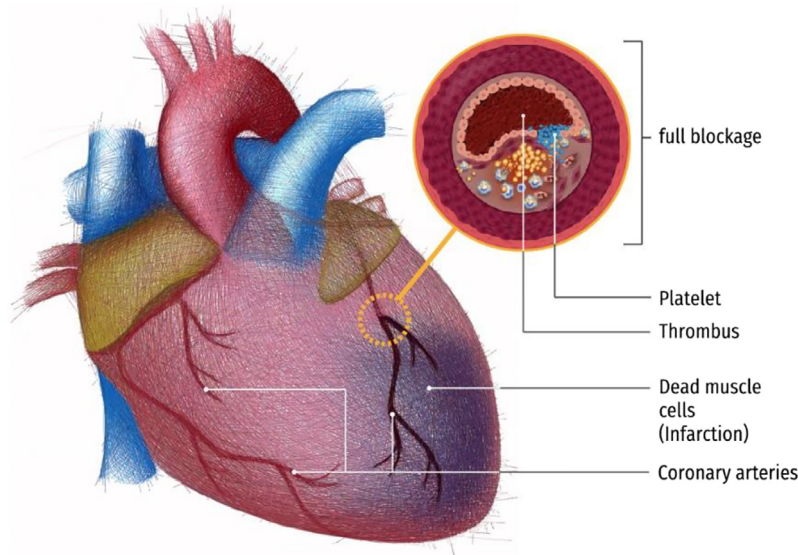 E-mail address: HFujita-799@acm.org (H. Fujita).

Fig. 1. An illustration of myocardial infarction.

tack [26]. Hence, approximately 72% of the heart attacks are silent. In other words, 72% of the patients' heart muscles are damaged but they are not aware of it. As a result, the mortality rate of MI is very high.

Therefore, an early diagnosis of MI will help patients to get timely treatment, and hence decreasing the prevalence of mortality [2]. The death of the heart muscles is irreversible hence, it is essential to get diagnosed early. The early diagnosis of MI can be conducted with an electrocardiogram (ECG). The ECG is the noninvasive economical primary tool which can be used to diagnose the cardiac abnormalities [4]. Fig. 2 shows the samples of normal and MI ECG signals with and without the removal of noise.

However, the ECG signals are having a very small amplitude (mV) and small duration (sec). Hence, the interpretation of these long duration of signals may lead to inter and intra-observer variabilities [25]. Moreover, it is time-consuming and strenuous to analyze the ECG signals.

The limitation of manual inspection of ECG signals can be overcome by using computer-aided diagnosis system [9]. A computer-aided diagnosis (CAD) system is preferred due to its fast, objective, and reliable analysis [9]. Many works have been conducted on the development of CAD for MI [1,18].

The studies presented in Table 6 have denoised their ECG signals before performing any feature extraction [2,5,6,22,24,31,33,35]. Nevertheless, denoising is not required in our proposed algorithm. Our algorithm can detect MI ECG signal without filtering any noise present in the ECG signal. Various features extraction techniques have been proposed to automatically detect MI using ECG signals. However, the process of choosing a set of optimal features to classify normal and MI ECG signals is very difficult [10].

Therefore, deep learning technique is introduced in this work to overcome the challenges faced by conventional automated systems. Recently, deep learning techniques have been used by many companies namely Adobe, Apple, Baidu, Facebook, Google, IBM, Microsoft, NEC, Netflix, and NVIDIA [12]. In our work, we have used an eleven layer deep CNN for the classification.

Deep learning is a representation based learning which consists of an input layer, hidden layers, and an output layer [23]. A representation based learning is a set of systematic procedures that provides a network to be fed with raw data and automatically learns the necessary representations for classification. The term deep describes the multiple stages in the learning process of the network structure [23]. The deep learning neural network is trained using the backpropagation algorithm. The CNN is one of the most popular neural network techniques [13].

CNN has been successfully utilized in computer vision since the early 21st century [23]. It performed well in recognizing handwritten digits, detecting objects, and speech recognition [23]. It has been used in the medical research field such as analyzing health informatics [30], and medical images [36] using computed tomography (CT) images [32], fundus images [14,15,37], histopathological images [16], magnetic resonance (MR) images [29], and X-ray images [19] as well. It is also noted that researchers in the medical analysis field are moving into CNN and obtaining desirable results [13]. Furthermore, we applied CNN in our previous work [3]. Our proposed system achieved the highest accuracy of *92.50%* and *94.90%* in the detection of arrhythmias with *two* and *five* seconds ECG signal [3]. Hence, the CNN has performed well in the biomedical signal and image processing domain. So, in this work, we employed it for the automated diagnosis of MI using ECG signals with and without noise.
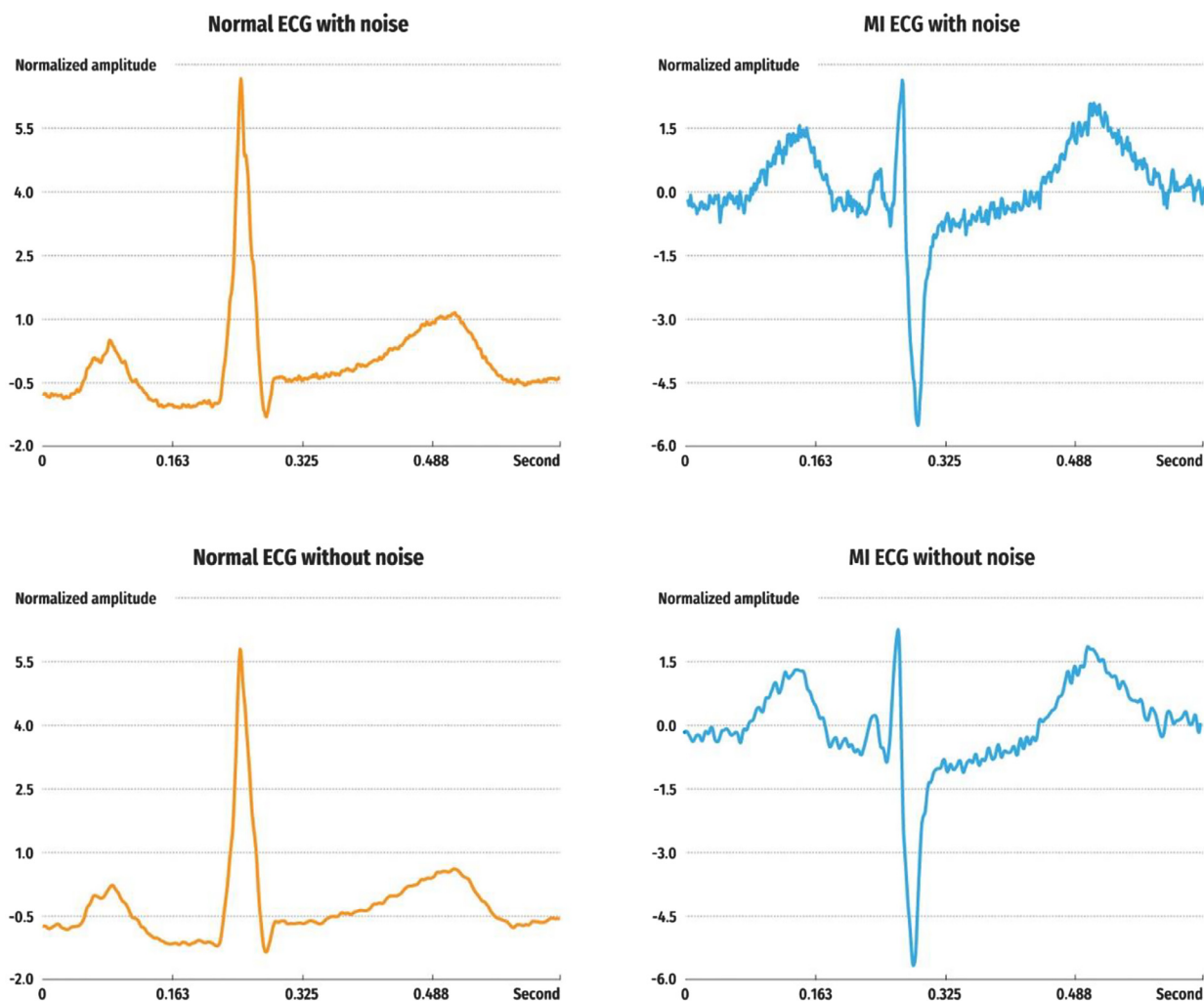
Fig. 2. Sample normal and MI ECG beat with and without noise removal.

Table 1
The characteristics of the ECG data obtained from PTB database.

	Normal	MI
Minimum age	17	36
Maximum age	81	86
Average age	43.43	60.37
Number of male	39	110
Number of female	13	38

2. Data used

In this work, the ECG signals were obtained from the ECG database (Physikalisch-Technische Bundesanstalt diagnostic ECG database) [11]. This database provides ECG data of 200 subjects (148 MI and 52 healthy subjects). Also, *12* leads signals were recorded from each subject. In our present work, we have used only lead II. Table 1 presents the characteristics of the ECG data obtained from PTB database.

Each signal is sampled at 1000 samples per second. We have used a total of 10,546 normal ECG beats and 40,182 MI ECG beats for this study. Each ECG beat consists of 651 samples comprising of one P-QRS-T wave.
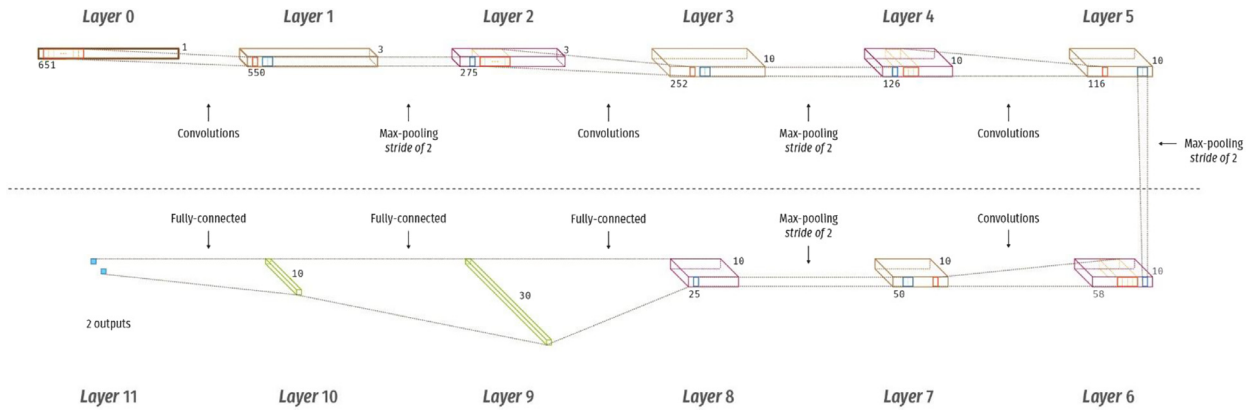
Fig. 3. The architecture of the proposed CNN.

Table 2
The details of CNN structure for noise and without noise ECG data.

Layers	Type	Number of neurons (Output Layer)	Kernel size for each output feature map	Stride
0–1	Convolution	550×3	102	1
1–2	Max-pooling	275×3	2	2
2–3	Convolution	252×10	24	1
3–4	Max-pooling	126×10	2	2
4–5	Convolution	116×10	11	1
5–6	Max-pooling	58×10	2	2
6–7	Convolution	50×10	9	1
7–8	Max-pooling	25×10	2	2
8–9	Fully-connected	30	–	–
9–10	Fully-connected	10	–	–
10–11	Fully-connected	2	–	–

3. Methodology

3.1. Pre-processing

In this work, we validate our proposed method with two sets of ECG data. Both datasets consist of the same number of ECG beats. However, in one of the dataset, we denoised and removed the baseline wander from the ECG signal using Daubechies wavelet *6* mother wavelet function [34]. But, in the other dataset, we retained the noises present in the ECG signals. Then, we carried out the R-peak detection on both datasets (with and without noise) using Pan Tompkins algorithm [28].

All the ECG signals are segmented using the detected R-peaks without the inclusion of the first and last beat. Each segment is normalized with Z-score normalization to address the problem of amplitude scaling and eliminate the offset effect before feeding the ECG segments into the *1*-dimensional deep learning CNN for training and testing. Each ECG beat consists of 651 samples (250 samples before R-peaks detection and 400 samples after R-peaks detection). Typical ECG beat with and without noise used in this study is shown in Fig. 2.

3.2. The architecture

The standard architecture of a CNN consists of *four* stages (i) Convolution, (ii) Rectified linear activation function, (iii) Pooling function, and (iv) Fully connected layer [12,23]. Fig. 3 shows a graphical representation of the architecture of our proposed system. Table 2 summarizes the details of the CNN structure used in this work.

(i) **Convolution layer**

The convolution layer is the main building block of a CNN. This layer does most of the computational intensive lifting. The prime objective of convolution is to extract features from the input ECG signals. The convolution layers are arranged in feature maps [23] (11 layers of feature maps in total).

(ii) **Rectified linear activation function**

In general, rectified linear activation serves to map nonlinearity into the data [23]. In this work, the leaky rectifier linear unit (LeakyRelu) [17] is used as an activation function for layers 1, 3, 5, 7, 9, and 10. Also, the softmax function is implemented for layer 11 (last layer).
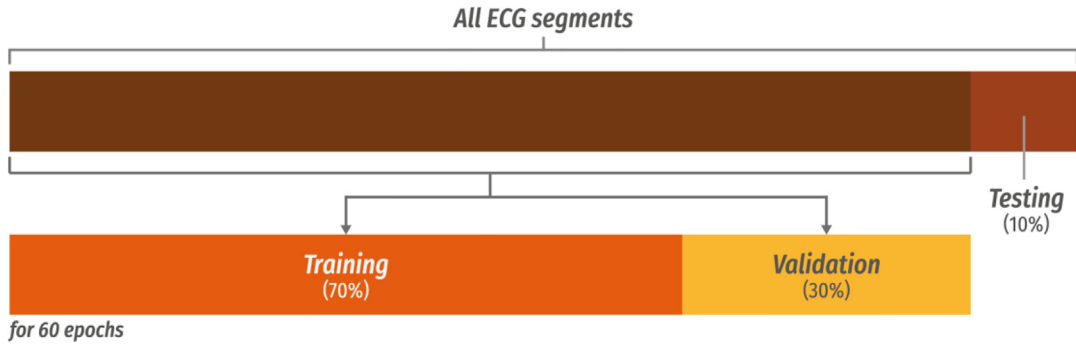
Fig. 4. The apportion of ECG beats used for training and testing the proposed algorithm.

(iii) **Pooling function**

Pooling also referred to as downsampling which is an operation to condense features and computational complexity of the network. The max-pooling operation is employed in this work. Max-pooling outputs only the maximum number in each kernel, thus reducing the feature map size [23].

Kernel size also refers to the size of the filter which convolves around the feature map while stride controls how the filter convolves around the feature map [23]. The amount by which the filter slides is the stride. In this work, the stride is set at 1. Therefore, the filter convolves around the different layers of feature map by sliding one unit each time.

(iv) **Fully connected layer**

The final layer of the fully-connected network is a softmax layer with an output of X dimensional vector where X is the number of classes that we desire to have. In this study, it is a two-class (normal and MI ECG signals) problem, hence, X is set at 2 in this work.

The input layer (layer *0*) is convolved with a kernel size of 102 to form the first layer (layer 1). After which, a max-pooling of size 2 is applied to every feature map (layer *2*). After performing the max-pooling operation, the number of neurons reduces from 550×3 to 275×3. Then the feature map from layer 2 is convolved with a kernel (filter of size 24) to form layer 3. A max-pooling is again applied to every feature map (layer 4). After that, a feature map from layer 4 is convolved with a filter of size 11 to produce layer 5. A max-pooling of size 2 is applied to every feature map to reduce the number of neurons to 58×10 (layer 6). Subsequently, the feature map in layer 6 is convolved with a kernel (filter of size 9) to form layer 7. A max-pooling is once again performed (layer 8). Finally, in layer 8, the neurons are fully connected to 30 neurons in layer 9. Layer 9 is connected to 10 neurons in layer 10. Layer 10 is connected to the last layer with 2 output neurons.

3.2.1. Training

A standard backpropagation [7] with a batch size of 10 is executed in this work. The regularization, momentum, and learning rate parameters are set to 0.2, 3×10^{-4}, and 0.7 respectively. These parameters are tuned accordingly to obtain optimum performance. The function of these parameters are as follows [20]:

a. Regularization: To prevent overfitting of the data.
b. Momentum: To control how fast or slow the network learn during training.
c. Learning rate: To help in the convergence of the data.

3.2.2. Testing

In this work, we ran a total of *60* epochs of training and testing rounds. At the end of every epoch, our proposed algorithm validates the CNN model. Out of the $\frac{9}{10}$ training ECG beats, we used $\frac{7}{10}$ to validate our proposed algorithm. Fig. 4 shows the apportioning of the total ECG beats for training and testing purposes.

3.3. k-fold cross-validation

We have employed a *10*-fold cross-validation [8] strategy in this work. We separated our total ECG beats almost equally into *10* segments. $\frac{9}{10}$ ECG beats are used in the training of CNN while the remainder ($\frac{1}{10}$) of the ECG beats are used to validate the performance of our proposed system. This approach is iterated *10* times by shifting the test data. The performances (accuracy, sensitivity, and specificity) are evaluated in each iteration. Finally, the performances recorded in all *10* iterations are averaged and considered as the overall performance of our proposed system.

Table 3
Confusion matrix of ECG beats with noise across *10*-folds.

		Predicted		ACC (%)	PPV (%)	SEN (%)	SPEC (%)
		Normal	MI				
Original	Normal	9790	756	93.53	79.48	92.83	93.71
	MI	2527	37,655	93.53	98.03	93.71	92.83

ACC = Accuracy, PPV = Positive Predictive Value, SEN = Sensitivity, SPEC = Specificity

Table 4
Confusion matrix of ECG beats without noise across *10*-folds.

		Predicted		ACC (%)	PPV (%)	SEN (%)	SPEC (%)
		Normal	MI				
Original	Normal	9933	613	95.22	84.56	94.19	95.49
	MI	1814	38,368	95.22	98.43	95.49	94.19

ACC = Accuracy, PPV = Positive Predictive Value, SEN Sensitivity, SPEC = Specificity

Table 5
The overall classification results for the classification of normal and MI classes across *10*-folds.

Beats Type	*TP*	*TN*	*FP*	*FN*	ACC (%)	PPV (%)	SEN (%)	SPEC (%)
Noise	37,655	9790	756	2527	93.53	98.03	93.71	92.83
Without Noise	38,368	9933	613	1814	95.22	98.43	95.49	94.19

TP = True Positive, *TN* = True Negative, *FP* = False Positive, *FP* = False Negative
ACC = Accuracy, PPV = Positive Predictive Value, SEN = Sensitivity, SPEC = Specificity

4. Results

In this study, we trained our algorithm on a workstation with two Intel Xeon 2.40 GHz (E5620) processor and a 24GB RAM. It typically took approximately 2151.055 s to complete an epoch of training for ECG beats data with noise and 2025.178 s for ECG beats data without noise.

The confusion matrix for ECG beats with noise and without noise are presented in Tables 3 and 4 respectively. It can be observed from Table 3 that, out of 10,546 normal ECG beats, approximately 7.17% of the ECG beats are wrongly classified as MI. Likewise, for MI, a total of 6.29% of ECG beats are wrongly classified as normal ECG beats. Similarly, in Table 4, 94.19% of ECG beats are correctly classified as normal ECG beats and 4.51% are wrongly classified as normal ECG beats.

Furthermore, the PPV values for each class (normal and MI) are recorded in Tables 3 and 4. In Table 3, the PPV in the normal class is 79.48% whereas the PPV in the MI class is 98.03%. This shows that the probability of correctly detecting the MI ECG signals from the ECG signals is higher as compared to the correct detection of normal ECG signals. Similarly, in Table 4, the PPV in the normal and MI classes are 84.56% and 98.43% respectively. This also shows that the probability of identifying MI ECG signals is higher than the identification of normal ECG signals in the ECG signals with noise removal.

The performance rate of both ECG beats with and without noise are summarized in Table 5. An average accuracy, sensitivity, and specificity of 93.53%, 93.71%, and 92.83% are achieved using ECG beats with noise introduced respectively. Furthermore, the highest average accuracy of 95.22% sensitivity of 95.49% and specificity of 94.19% is obtained for ECG beat without noise.

5. Discussion

Table 6 summarizes the various techniques employed by the researchers for automated detection of MI using ECG signals obtained from the same public database (PTBDB). However, not all studies are performed with lead II ECG signals. The majority of the researchers used *12* leads ECG signals in their studies [2,5,22,24,33,35]. In our previous study [2], we have used all 12 leads ECG signals to compare the results of the different leads. Banerjee et al. [6] conducted a study with lead III ECG signals. They have used lead III in their work and found morphological differences in MI and normal ECG signals in the QT zone. We have used lead II in this study as it is a commonly used lead for basic cardiac monitoring. Further, lead II can provide good ECG morphological information.

It can be noted from Table 6 that the proposed system performed better using the ECG beats without noise. Normally, noise is unwanted information present in the signal [38]. Hence, the noise present in the ECG beats reduces the overall performance of the proposed system. Nevertheless, we achieved comparable results for both with and without noise ECG beats. Therefore, this proves that our proposed method is robust to noise. This also implies that our proposed CNN model can understand the underlying structure of noisy ECG beat. Thus, we might be able to accurately classify the unknown noisy ECG beat with our proposed system.

Table 6

Summary of selected studies conducted for the detection and diagnosis of MI using ECG signals obtained from PTBDB.

Author, Year	Number of Leads	Notable features	Number of ECG beats	Classifier used	Performance
Lahiri et al., 2009 [22]	12 leads	• R-peaks detection • Phase space fractal dimension of ECG	64,680 R-peaks from 1848	Artificial neural network	$Eff = 96.00\%$
Banerjee et al., 2012 [6]	lead III	• R-peaks detection • Cross wavelet transform • Wavelet coherence technique	Normal: 1 148 MI patients	–	ECG patterns portray distinct difference over regions R1 and R2
Arif et al., 2012 [5]	12 leads	• QRS detection • Time-domain features	Normal: 3200 MI: 16,960	k-nearest neighbor	$Sen = 99.97\%$ $Spec = 99.90\%$
Sun et al., 2012 [35]	12 leads	• ST detection • Multiple instance learning	Normal: 79 records MI: 369 records	Support vector machine	$Sen = 92.60\%$ $Spec = 82.40\%$
Safdarian et al., 2014 [31]	lead II	• T-wave detection • Artificial neural network	549 records	Naïve Bayes	$Acc = 94.74\%$
Liu et al., 2015 [24]	12 leads	• R-peaks detection • ECG polynomial fitting (polyfit) • Polyfit-based ECG parameterization • Akaike information criterion	Normal: 52 subjects MI: 148 patients	J48 decision tree	$Acc = 94.40\%$
Sharma et al., 2015 [33]	12 leads	• Wavelet transform • Multiscale energy • Multiscale eigenspace analysis	549 records	Support vector machine	$Acc = 96.00\%$ $Sen = 93.00\%$ $Spec = 99.00\%$
Acharya et al., 2016 [2]	12 leads	• R-peaks detection • MI detection with 47 features| • MI localization with 25 features	Normal: 125,652 MI: 485,753	k-nearest neighbor	$Acc = 98.80\%$ $Sen = 99.45\%$ $Spec = 96.27\%$
In this study	**lead II**	**• R-peaks detection** **• 11-layer deep neural network** **• No feature selection or feature reduction** **• Denoising not required**	**Normal: 10,546** **MI: 40,182**	**Convolutional neural network**	**With noise:** $Acc = 93.53\%$ $Sen = 93.71\%$ $Spec = 92.83\%$ **Without noise:** $Acc = 95.22\%$ $Sen = 95.49\%$ $Spec = 94.19\%$

Acc = Accuracy, Eff = Efficiency, Sen = Sensitivity, $Spec$ = Specificity

MI = myocardial infarction

PTBDB = Physikalisch-Technische Bundesanstalt database

The performance of our proposed system is comparable to the performances presented in Table 6. In our work, we have used deep learning method. Hence, the CNN need not perform the feature extraction and selection process in signal analysis. This is the advantage of deep learning over the traditional machine learning algorithms. Thus, we need not experiment with different types of feature extraction or feature selection techniques. We are also not required to manually develop an optimum set of features to be fed into the classifiers. Also, the performance of our proposed method will improve with the number of data. Big data is required to train our proposed system for better performance.

The main highlights of our proposed algorithm are as follows:

 i. Feature extraction and selection techniques are not needed.
 ii. *11*-layer deep CNN is implemented.
iii. *10*-fold cross-validation is done in this work, hence increasing the robustness of the system.
iv. Denoising is not required.

The drawbacks of our proposed algorithm are as follows:

 i. It is computationally intensive to learn the features.
ii. It requires a huge diverse of data.

In fact, the long training time is secondary, if our proposed system can classify normal and MI classes accurately. Furthermore, once our proposed system is trained, the system can identify an unknown ECG beat immediately. Moreover, given that CNNs are concurrently-based algorithms, training the CNNs with graphics processing unit (GPU) will help to reduce the complexity and power consumption due to computation.

As part of our future study, we intend to boost the performance and reliability of our proposed system by applying bagging algorithm in our next work and to obtain more ECG data from other open source databases. We also intend to extend this approach to other cardiovascular diseases such as heart failure, hypertensive heart disease, cardiomyopathy.

Conclusion

The early diagnosis of MI can save life and can help to provide timely treatment. Thus, it is necessary to go for annual health checkups. The ECG is the primary tool to diagnose the electrical activity of the heart. Any abnormalities present in the heart activity is reflected in the ECG signals. However, it is challenging and time-consuming to visually assess the ECG signals. Therefore, implementing a CAD system in clinical settings will ensure an objective and fast diagnosis of MI. In this work, we proposed a novel method to automatically diagnose MI using *11*-layer deep CNN. We have used *two* different datasets (with and without noise) to evaluate the effectiveness of our proposed method. We have achieved an average accuracy, sensitivity, and specificity of 93.53%, 93.71%, and 92.83% respectively for ECG beats with noise. Our proposed system attained high-performance results even though there are noises present in the ECG beats. This suggests that our system can recognize the class of the ECG signals even with the presence of noise in the signal. Also, we obtained an average accuracy, sensitivity, and specificity of 95.22%, 95.49%, and 94.19% for ECG beats without noise. This shows that the overall performance of our proposed system is good enough and hence, can be introduced in clinical settings. Our proposed system can assist doctors in their diagnosis.

References

[1] U.R. Acharya, H. Fujita, A. Muhammad, S.L. Oh, V.K. Sudarshan, J.H. Tan, J.E.W. Koh, Y. Hagiwara, K.C. Chua, K.P. Chua, R.S. Tan, Automated characterization and classification of coronary artery disease and myocardial infarction by decomposition of ECG signals: a comparative study, Inf. Sci. 337 (2017) 17–29.
[2] U.R. Acharya, H. Fujita, V.K. Sudarshan, S.L. Oh, M. Adam, J.E.W. Koh, J.H. Tan, D.N. Ghista, R.J. Martis, K.C. Chua, K.P. Chua, R.S. Tan, Automated detection and localization of myocardial infarction using electrocardiogram: a comparative study of different leads, Knowl.-Based Syst. 99 (2016) 146–156.
[3] U.R. Acharya, H. Fujita, S.L. Oh, Y. Hagiwara, J.H. Tan, A. Muhammad, Automated detection of arrhythmias using different intervals of tachycardia ecg segments with convolutional neural network, Inf. Sci. 405 (2017) 81–90.
[4] U.R. Acharya, N. Kannathal, M.H. Lee, M.Y. Leong, Study of heart rate variability signals at sitting and lying postures, J. Body Mov. Ther. 9 (2005) 134–141.
[5] M. Arif, I.A. Malagore, F.A. Afsar, Detection and localization of myocardial infarction using K-nearest neighbor classifier, J. Med. Syst. 36 (2012) 279–289.
[6] S. Banerjee, M. Mitra, Cross wavelet transform based analysis of electrocardiogram signals, Int. J. Electr., Electron. Comput. Eng. 1 (2) (2012) 88–92.
[7] J. Bouvrie, Notes on convolutional neural network, 2007.
[8] R.O. Duda, P.E. Hart, D.G. Stork, Pattern Classification, 2nd edition, John Wiley and Sons, New York, 2001.
[9] O. Faust, U.R. Acharya, T. Tamura, Formal design methods for reliable computer-aided diagnosis: a review, IEEE Rev. Biomed. Eng. 5 (2012) 15–28.
[10] B.V. Ginneken, Fifty years of computer analysis in chest imaging: rule-based, machine learning, deep learning, Radiol. Phys. Technol. 10 (1) (2017) 23–32.
[11] A.L. Goldberger, L.A.N. Amaral, L. Glass, J.M. Hausdorff, P.C.H. Ivanov, R.G. Mark, J.E. Mietus, G.B. Moody, C.K. Peng, H.E. Stanley, PhysioBank, PhysioToolkit, and PhysioNet: components of a new research resource for complex physiologic signals, Circulation 101 (23) (2000) e215–e220.
[12] I. Goodfellow, Y. Bengio, A. Courville, Deep Learning, MIT Press, 2016 http://www.deeplearningbook.org.
[13] H. Greenspan, R.M. Summers, B. van Ginneken, Deep learning in medical imaging: overview and future promise of an exciting new technique, IEEE Trans. Med. Imaging 35 (5) (2016) 1153–1159.
[14] M.J.J.P. van Grinsven, B. van Grinneken, C.B. Hoyng, T. Theelen, C.I. Sánchez, Fast convolutional neural network training using selective data sampling: application to hemorrhage detection in color fundus images, IEEE Trans. Med. Imaging 35 (5) (2016) 1273–1284.
[15] V. Gulshan, L. Peng, M. Coram, M.C. Stumpe, D. Wu, A. Narayanaswamy, S. Venugopalan, K. Widner, T. Madams, J. Cuadros, R. Kim, R. Raman, P.C. Nelson, J.L. Mega, D.R. Webster, Development and validation of a deep learning algorithm for detection of diabetic retinopathy in retinal fundus photographs, JAMA 16 (22) (2016) 2402–2410.
[16] N. Hatipoglu, G. Bilgin, Cell segmentation in histopathological images with deep learning algorithms by utilizing spatial relationships, Med. Biol. Eng. Comput. (2017) 1–20, doi:10.1007/s11517-017-1630-1.
[17] He.K. Zhang, X. Ren, S. Sun, Delving deep into rectifiers: surpassing human-level performance on image net classification, 1026–1034, 2015.
[18] E.S. Jayachandran, K.P. Joseph, U.R. Acharya, Analysis of myocardial infarction using discrete wavelet transform, J. Med. Syst. 34 (2010) 985–992.
[19] M. Kallenberg, K. Petersen, M. Nielsen, Y.A. Ng, P.F. Diao, C. Igel, C.M. Vachon, K. Holland, R.R. Winkel, N. Karssemeijer, M. Lillholm, Unsupervised deep learning applied to breast density segmentation and mammographic risk scoring, IEEE Trans. Med. Imaging 35 (5) (2016) 1322–1331.
[20] A. Krizhevsky, I. Sutskever, G.E. Hinton, ImageNet classification with deep convolutional neural networks, Neural Information Processing Systems Conference, 25, 2012.
[21] D.K Kulick, J.W. Marks, C.P. Davis, Heart Attack (Myocardial Infarction), 2015. Retrieved from http://www.medicinenet.com/heart_attack/article.htm.
[22] T. Lahiri, U. Kumar, H. Mishra, S. Sarkar, A.D. Roy, Analysis of ECG signal by chaos principle to help automatic diagnosis of myocardial infarction, J. Scient. Industr. Res. 68 (2009) 866–870.
[23] Y. LeCun, Y. Bengio, G. Hinton, Deep learning, Nature 521 (2015) 436–444.
[24] B. Liu, J. Liu, G. Wang, K. Huang, F. Li, Y. Zheng, Y. Luo, F. Zhou, A novel electrocardiogram parameterization algorithm and its application in myocardial infarction detection, Comput. Biol. Med. 61 (2015) 178–184.
[25] R.J. Martis, U.R. Acharya, H. Adeli, Current methods in electrocardiogram characterization, Comput. Biol. Med. 48 (2014) 133–149.
[26] E. Mozaffarian, E.J. Benjamin, A.S. Go, D.K. Arnett, M.J. Blaha, M. Cushman, S.R. Das, S. de. Ferranti, J.P. Després, H.J. Fullerton, V.J. Howard, M.D. Huffman, C.R. Isasi, M.C. Jiménez, S.E. Judd, B.M. Kissela, J.H. Lichtman, L.D. Lisabeth, S. Liu, R.H. Mackey, D.J. Magid, D.K. McGuire, E.R. Mohler, C.S. Moy, P. Muntner, M.E. Mussolino, K. Nasir, R.W. Neumar, G. Nichol, L. Palaniappan, D.K. Pandey, M.J. Reeves, C.J. Rodriguez, W. Rosamond, P.D. Sorlie, J. Stein, A. Towfighi, T.N. Turan, S.S. Virani, D. Woo, R.W. Yeh, M.B Turner, Heart disease and stroke statistics–2016 update, Circulation (2016).
[27] National Heart, Lung, and Blood Institute, What is a Heart Attack, 2015. Retrieved from https://www.nhlbi.nih.gov/health/health-topics/topics/heartattack/.
[28] J. Pan, W.J. Tompkins, A real-time QRS detection algorithm, IEEE Trans. Biomed. Eng. 32 (3) (1985) 230–236.
[29] S. Pereira, A. Pinto, V. Alves, C.A. Silva, Brain tumor segmentation using convolutional neural networks in MRI images, IEEE Trans. Med. Imaging 35 (5) (2016) 1240–1251.
[30] D. Ravi, C. Wong, F. Deligianni, M. Berthelot, J. Andreu-Perez, B. Lo, G.Z. Yang, Deep leaning for health informatics, IEEE J. Biomed. Health Inform. 21 (1) (2017) 4–21.

[31] N. Safdarian, N.J. Dabanloo, G.A Attarodi, New pattern recognition method for detection and localization of myocardial infarction using t-wave integral and total integral as extracted features from one cycle of ECG signal, J. Biomed. Sci. Eng. 7 (10) (2014) 818–824.

[32] A.A.A. Setio, F. Ciompi, G. Litjens, P. Gerke, C. Jacobs, S.J. van Riel, M.M.W. Wille, M. Naqibullah, C.I. Sánchex, B. van Ginneken, Pulmonary nodule detection in CT images: false positive reduction using multi-view convolutional networks, IEEE Trans. Med. Imaging 35 (5) (2016) 1160–1169.

[33] L.N. Sharma, R.K. Tripathy, S. Dandapat, Multiscale energy and eigenspace approach to detection and localization of myocardial infarction, IEEE Trans. Biomed. Eng. 62 (7) (2015) 1827–1837.

[34] V. Singh, A. Tiwari, Optimal selection of wavelet basis function applied to ECG signal denoising, Digital Signal Process. 16 (3) (2006) 275–287.

[35] L. Sun, Y. Lu, K. Yang, S. Li, ECG analysis using multiple instance learning for myocardial infarction detection, IEEE Trans. Biomed. Eng. 59 (12) (2012) 3348–3356.

[36] N. Tajbakhsh, J.Y. Shin, S.R. Gurundu, R.T. Hurst, C.B. Kendall, M.B. Gotway, J.M. Liang, Convolutional neural networks for medical image analysis: full training or fine tuning, IEEE Trans. Med. Imaging 35 (5) (2016) 1299–1312.

[37] J.H. Tan, U.R. Acharya, S.V. Bhandary, K.C. Chua, S. Sivaprasad, Segmentation of optic disc, fovea, and retinal vasculature using a single convolutional neural network, J. Comput. Sci. (2017), doi:10.1016/j.jocs.2017.02.006.

[38] V. Tuzlukov, Signal Processing Noise Electrical Engineering, and Applied Signal Processing Series, CRC Press, 2010.